about 1.″2, the true spectral resolution is around 8 Å, consistent with the measured width of the spectral features. The average line profile, constructed from the Fe II lines above 6000 Å, appears unresolved. This implies that the absorbing clouds have a velocity dispersion of less than 100 km s^{-1} in the rest frame.

The observed BATSE gamma-ray fluence of GRB 990123 is $5.09 \pm 0.02 \times 10^{-4}$ erg cm^{-2} for energies above 20 keV [14]. In Table 2 we give the luminosity distance and the inferred isotropic energy output in various cosmologies for $z = 1.600$. A lower limit to the isotropic energy release in gamma-rays alone is obtained in an Einstein-de Sitter Universe with $(\Omega_0 \Omega_\Lambda) = (1,0)$. For a upper limit to the Hubble constant of $H_0 < 80$ km s^{-1} Mpc^{-1} we find a lower limit of 0.5 times the rest mass of a neutron star (1.4 M$_\odot$ = 2.5×10^{54} erg) or ~2.5 times its binding energy. For a set of currently observationally favored cosmological parameters $(\Omega_0 \Omega_\Lambda) = (0.2, 0.8)$ and $H_0 = 65$ km s^{-1} Mpc^{-1} we derive an energy release in gamma-rays equivalent to 1.8 neutron stars. This is 45 times larger than the total energy emitted in all wavelengths by the most luminous Type II supernova, including neutrino emission [15].

If the GRB 990123 is located at $z > 1.6$ our upper limit on z translates into an upper limit on the energy release of 1.3×10^{55} erg for $H_0 > 50$ km s^{-1} Mpc^{-1} and $(\Omega_0 \Omega_\Lambda) = (0.2, 0.8)$. Moreover, if the $z = 1.6$ absorption system is associated with the main mass component along the line of sight to GRB 990123, the upper limit on z leads to a required lensing surface mass density of a factor of about three to four times that in normal galaxy lenses. This effectively rules out the possibility that GRB 990123 was lensed (multiply imaged) [16] by this mass.

Any of the above numbers indicates a huge isotropic energy release which is difficult to reconcile with current physical theories. In the absence of lensing one resolution of this energy problem is that the gamma-ray emission from GRB 990123 was not isotropic. This interpretation is consistent with polarimetric observations [17] and is supported by the breaks observed in the light curve [5, 8, 12] which suggest that the optical afterglow may have been beamed.

References and Notes

1. G. J. Fishman and C. A. Meegan, *Annu. Rev. Astron. Astrophys.* **33**, 415 (1995).
2. M. R. Metzger *et al.*, *Nature* **387**, 879 (1997); S. R. Kulkarni *et al.*, *ibid.* **393**, 35 (1998); S. G. Djorgovski *et al.*, *Astrophys. J.* **507**, L25 (1998).
3. J. Heise, in preparation.
4. S. C. Odewahn, J. S. Bloom, S. R. Kulkarni, *GCN Circular 201* (1999); *IAU Circular 7094* (1999).
5. S. R. Kulkarni *et al.*, *Nature*, in press, preprint also available at http://www.lanl.gov/abs/astro-ph/9902272.
6. C. W. Akerlof and T. A. McKay, *GCN Circular 205* (1999); *IAU Circular 7100* (1999); *Nature*, in press.
7. A more comprehensive analysis of the absorption system will be presented in a paper in preparation.
8. A. J. Castro-Tirado *et al.*, *Science* **283**, 2069 (1999).
9. P. Møller and P. Jakobsen, *Astron. Astrophys.* **228**, 299 (1990).
10. M. Pettini, D. L. King, L. J. Smith, R. W. Hunstead, *Astrophys. J.* **478**, 536 (1997); M. Pettini, L. J. Smith, D. L. King, R. W. Hunstead, *ibid.* **486**, 665 (1997).
11. J. S. Bloom *et al.*, in preparation, preprint available at http://www.lanl.gov/abs/astro-ph/9902182.
12. A. S. Fruchter *et al.*, in preparation, preprint available at http://www.lanl.gov/abs/astro-ph/9902236.
13. S. Holland and J. Hjorth, *Astron. Astrophys.*, in press, preprint also available at http://www.lanl.gov/abs/astro-ph/9903175.
14. R. M. Kippen, *GCN Circular 224* (1999).
15. See *Thermonuclear Supernovae*, P. Ruiz-Lapuente, R. Canal, J. Isern, Eds. (Kluwer Academic, Dordrecht, Netherlands, 1997).
16. S. G. Djorgovski *et al.*, *GCN Circular 216* (1999).
17. J. Hjorth *et al.*, *Science* **283**, 2073 (1999).
18. We thank the NOT director for continued support to our GRB programme. This research was supported by the Danish Natural Science Research Council (SNF), the Icelandic Council of Science and the University of Iceland Research Fund. The Nordic Optical Telescope is operated on the island of La Palma jointly by Denmark, Finland, Iceland, Norway, and Sweden in the Spanish Observatorio del Roque de los Muchachos of the Instituto de Astrofísica de Canarias. The data presented here have been taken using ALFOSC, which is owned by the Instituto de Astrofísica de Andalucía (IAA) and operated at the Nordic Optical Telescope under agreement between IAA and the Astronomical Observatory of the University of Copenhagen.

23 February 1999; accepted 9 March 1999

A Simple Predictive Model for the Structure of the Oceanic Pycnocline

Anand Gnanadesikan

A simple theory for the large-scale oceanic circulation is developed, relating pycnocline depth, Northern Hemisphere sinking, and low-latitude upwelling to pycnocline diffusivity and Southern Ocean winds and eddies. The results show that Southern Ocean processes help maintain the global ocean structure and that pycnocline diffusion controls low-latitude upwelling.

The main oceanic pycnocline delineates the boundary between light, low-latitude surface waters and dense, abyssal waters whose properties are set in the high latitudes (Fig. 1A). The physical properties at work in the pycnocline and the flows driven by the pressure gradients associated with the pycnocline affect the transport of heat, salt, and nutrients through the ocean. Here I examine the relative importance of several key processes in setting the structure of the pycnocline. These are (i) vertical diffusion within the pycnocline, (ii) upwelling through the pycnocline in low latitudes, (iii) the conversion of light to dense water associated with the formation of North Atlantic Deep Water, (iv) Southern Ocean winds, and (v) Southern Ocean eddies. Previous scaling theories of the pycnocline [1] have only included the first three processes.

The western Atlantic Ocean contains a bowl of waters lighter than 1027.5 kg m^{-3} ~1000 m deep, with some upward deflection at the equator [2]. A tongue of fresh Antarctic Intermediate Water (AAIW) penetrates northward from the Southern Ocean and a tongue of salty North Atlantic Deep Water (NADW) moves southward. In the conceptual framework I propose (Fig. 1C), surface cooling in the Northern Hemi-

National Oceanic and Atmospheric Administration (NOAA) Geophysical Fluid Dynamics Laboratory and Atmospheric and Oceanic Sciences Program, Princeton University, Post Office Box CN710, Princeton, NJ 08544, USA. E-mail: gnana@splash.princeton.edu

sphere (NH) leads to the conversion of light water to dense water, which flows southward at a rate T_n. Some portion of this flux upwells within the Southern Ocean, where precipitation causes it to become lighter. This light water is then exported to the north at a rate T_s. That portion of the NH sinking flux that is not balanced by upwelling within the Southern Ocean upwells through the low-latitude pycnocline at a rate T_u. I have ignored deep flows associated with the Antarctic Bottom Water (AABW), assuming that they have little direct effect on the pycnocline as they are returned at mid-depth [3]. Instead I focus on the effect of Northern and Southern Hemisphere mode waters on the lower pycnocline.

These fluxes can be connected to the depth of the pycnocline, reducing the equations governing the large-scale oceanic circulation to a single cubic equation in the pycnocline depth D. The first step is to derive an expression for T_n, the NH sinking flux. It is common to assume that this flow is proportional to the density difference between the light and dense water $\Delta\rho$ [4]. Because northward flow of AAIW and the southward flow of NADW are essentially pressure-driven, there is a level of no motion between the two flows at which the velocities and hence the pressure gradients are negligible. The mass of water above the level of no motion is thus the same at all latitudes. Because the warm waters in low latitudes are less dense, they take up more volume and the surface height is higher at the equator than in high latitudes. This surface height difference will cause a pressure differ-

ence Δp within the water column

$$\frac{\Delta p}{\rho} \sim \Delta\rho gD/\rho = g'D \qquad (1)$$

where D is the depth of the light water and g' is the reduced gravity. According to classical boundary layer theory (5) this pressure difference will produce a frictional flow near the eastern or western boundary (4, 6)

$$A_h \frac{\partial^2 v}{\partial x^2} = \frac{1}{\rho}\frac{\partial p}{\partial y} \rightarrow \frac{A_h V}{L_m^2}$$

$$= A_h^{1/3}\beta^{2/3}V = \frac{Cg'D}{L_y^n} \qquad (2)$$

where V is the north-south velocity within the boundary layer, $L_m = (A_h/\beta)^{1/3}$ is the width of the frictional boundary layer L_y^n is the north-south distance over which the gradient in layer depth occurs, β is the north-south gradient of the Coriolis parameter, A_h is the eddy viscosity, and C is a constant that incorporates effects of geometry and boundary layer structure. The volume flux driven by such a circulation is then

$$T_n = \frac{Cg'D^2}{\beta L_y^n} = V \times D \times L_m \qquad (3)$$

The final expression is independent of the eddy viscosity.

The Southern Hemisphere (SH) is governed by different dynamics. Between 55°S and 63°S (Drake Passage latitudes) there is open water all around the globe above depths of about 2000 m. Here, frictional boundary currents are absent in the surface ocean. Instead, the principal flows are a northward mass flux (the Ekman transport) driven by the winds (7) and a return flow of light water associated with mesocale eddies. The net transport to the north is compensated by a deep pressure-driven flow of dense water along the flanks of submarine ridges (3). Suppose the eddy component can be represented by the parameterization of Gent and McWilliams (8), so that the eddy-induced transport velocity goes as $v_{eddy} = A_I \partial S/\partial z$, where $S \sim D/L_y^s$ is the slope of the upper layer in the north-south direction and A_I is a diffusion coefficient. Such a flow will act to reduce the north-south slope of the upper layer. The meridional mass transport then is given by

$$T_s = \left(\frac{\tau}{\rho f} - v_{eddy} \times D\right) \times L_x$$

$$= \left(\frac{\tau}{\rho f} - \frac{A_I D}{L_y^s}\right) \times L_x \qquad (4)$$

where τ is the wind stress in the Southern Ocean, f is the Coriolis parameter, and L_x is the circumference of the earth in Drake Passage latitudes.

The difference between T_n and T_s must upwell through the low-latitude pycnocline. In order to maintain the pycnocline structure, the upward advective flux of dense water
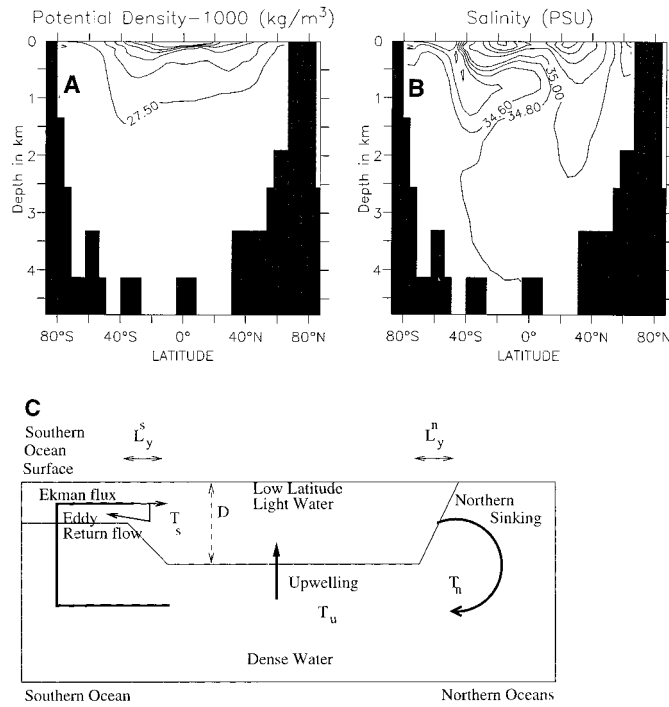

Fig. 1. (A) Average potential density referenced to 1000 m in the Atlantic Ocean. **(B)** Average salinity in the western Atlantic ocean. **(C)** Schematic of the flows which the simple theoretical model presented here assumes are responsible for the density and salinity structure.

must be balanced by a downward diffusive flux of heat by means of turbulent mixing. These fluxes can be related to the depth of the thermocline (9), $D = K_v A/T_u$ where K_v is the vertical diffusion coefficient and A is the surface area of the low-latitude box. The upwelling is the difference between T_n and T_s

$$T_u D = (T_n - T_s)D \rightarrow K_v A = \frac{Cg'}{L_y^n}D^3$$

$$+ \frac{A_I L_x}{L_y^s}D^2 - \frac{\tau L_x}{\rho f}D \qquad (5)$$

This equation represents the following two important balances:

1) If $T_s = 0$, the quadratic and linear terms are zero and the effect of Southern Ocean processes is neglected. Then the low-latitude upwelling (constant term) balances the NH sinking (cubic term). In this regime, the pycnocline depth goes as $(K_v/g')^{1/3}$ and the NH sinking goes as $K_v^{2/3}g'^{1/3}$. This is the scaling previously found (1) that has a strong dependence on vertical diffusivity. In this regime, the magnitude of the NH sinking depends solely on processes within the NH and pycnocline.

2) When the vertical diffusivity K_v and horizontal diffusivity A_I are vanishingly small, the constant and quadratic terms in Eq. 5 vanish. In this case, all the water that sinks in the north is supplied from the Southern Ocean so that there is a tight linkage between NH sinking (cubic term) and SH Ekman transport (linear term).

Southern Ocean eddies can substantially alter either scenario. The horizontal eddy exchange coefficient A_I has not been directly measured, although it has been estimated as being

between 100 and 3000 m² s⁻¹ (10). If it is large, a considerable amount of light water can be exported to the Southern Ocean within the near-surface layer. For other parameters held fixed, larger values of A_I would imply a thinner pycnocline and weaker NH sinking. If K_v is nonvanishing (but small), the low-latitude upwelling will be correlated with A_I.

For the data used to construct Fig. 1 we can estimate $g' = 0.01$ m s⁻², $L_y^n = L_y^s = 1500$ km, and a pycnocline depth of 570 m (11). Given that $\beta = 2 \times 10^{-11}$ m⁻¹ s⁻¹, $L_x = 25,000$ km, and $A = 2.44 \times 10^{14}$ m², in order to generate the observed overturning of around 17 Sv (12), $C = 0.16$ (within about 20%). A reasonable value of A_I is 1000 m² s⁻¹ (10). The dependence of the pycnocline depth, NH sinking, and overturning ratio T_s/T_n on SH wind stress and K_v can then be calculated from Eq. 5 (Fig. 2).

The observed pycnocline depth can be produced with low values of Southern Ocean wind stress and high values of vertical diffusion (0.6 cm² s⁻¹). This result agrees with models of ocean circulation in simple closed basins. However, such high values of vertical diffusion do not agree with observations (13); values of 0.1 to 0.15 cm² s⁻¹ seem to be more realistic. Such high values of K_v are also associated with large amounts of equatorial upwelling, which Toggweiler and Samuels (14) concluded was inconsistent with the observed radiocarbon field. The mismatch between the high values of K_v seemingly required by the numerical models and low values observed in the oceanic thermocline is often colloquially referred to as the "missing mixing problem" (15).

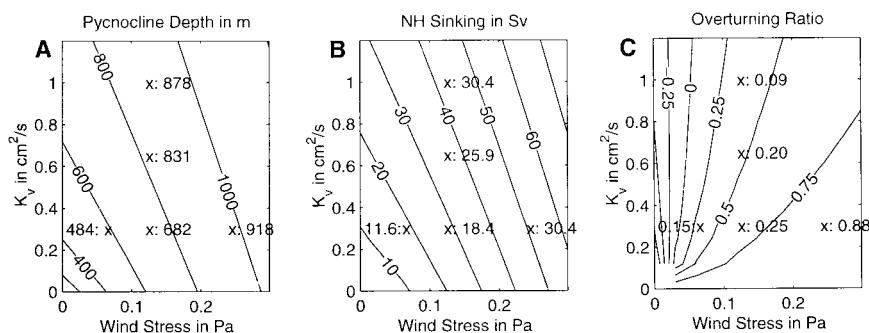The deeper thermocline can be produced

Fig. 2. Solutions to Eq. 5 as a function of Southern Ocean wind stress and vertical diffusivity within the pycnocline. Results from a general circulation model are superimposed as x symbols. (**A**) Pycnocline depth (in meters). (**B**) NH sinking T_n (in Sverdrups). (**C**) Overturning ratio T_s/T_n. This quantity represents the fraction of NH sinking supplied from the south. Negative values mean that there is net sinking in both NH and SH which is supplied from low-latitude upwelling.
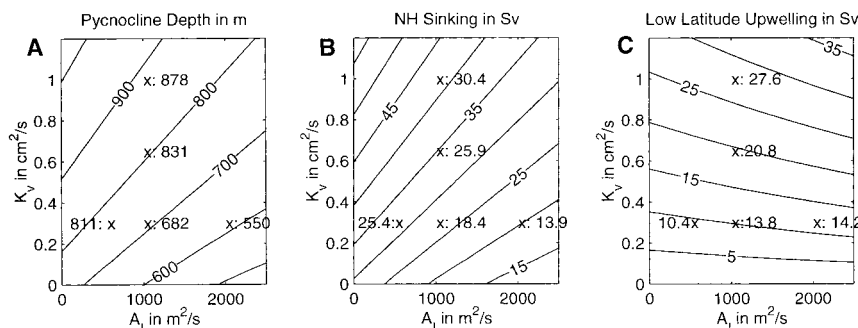

Fig. 3. Dependence of the (**A**) pycnocline depth (in meters) and (**B**) NH sinking and (**C**) equatorial upwelling (in Sverdrups) on A_I and K_v. Contours are from solving Eq. 5 with the coefficients as given in the text given a Southern Ocean wind stress of 0.12 Pa; x symbols are from a general circulation model.

without resorting to high levels of diffusion if Southern Ocean processes are taken into account (Fig. 2). As the Southern Ocean wind stress increases to more realistic values (0.1 to 0.2 Pa) the pycnocline depth, and thus the NH sinking, switches over to being primarily dependent on the SH winds and is relatively insensitive to the vertical diffusion. The low-latitude upwelling is very strongly dependent on the vertical diffusion and weakly dependent on the Southern Ocean winds. For the parameter values that are thought to govern the ocean at present (wind stresses of 0.1 to 0.2 Pa, vertical diffusivity of 0.1 to 0.15 cm^2 s^{-1}), the model predicts that most of the NH sinking is supplied from the Southern Ocean.

The solution is dependent on the parameterization of Southern Ocean eddies. As A_I increases, the pycnocline depth decreases and the low-latitude upwelling increases (Fig. 3). When A_I is very large, almost all of the NH sinking goes into low-latitude upwelling, so that the overturning ratio is small. When A_I is small most of the NH sinking does not upwell in low latitudes, and so the overturning ratio is large. This highlights the importance of understanding the dynamical effects of eddies in the Circumpolar Current.

Results from a general circulation model (GCM) (*16*) (symbols in Figs. 2 and 3) show a strong resemblance to the simple predictive model even though the simple model was intentionally not tuned to match the GCM. Both predict that as the SH winds increase, so do the depth of the pycnocline, magnitude of the NH sinking, and the portion of this sinking flux supplied from the SH (*14*, *17*). The theory does reasonably well quantitatively. For example, it explains the rough magnitude of the range in pycnocline depth versus A_I ($\sim$250 m) as well as the rough magnitude of the change in low-latitude upwelling versus K_v ($\sim$20 Sv). It also predicts the rough magnitude of the increase in thermocline depth with increases in Southern Ocean winds ($\sim$500 m). Analysis showed that the value of C that provided the best fit to the model (0.1) was smaller than that chosen from the data (0.16). Although the model predicts a systematically lower NH sinking (and hence overturning ratio) than the simple theory, the rough magnitude of the changes in sinking and overturning ratio with respect to wind stress, A_I, and K_v are reasonable.

References and Notes

1. F. Bryan, *J. Phys. Oceanogr.* **17**, 970 (1987); R. A. DeSzoeke, *ibid.* **25**, 918 (1995).
2. S. Levitus, *A Climatological Atlas of the World Ocean* (NOAA Prof. Pap. 13, U.S. Government Printing Office, Washington, DC, 1992).
3. See A. Macdonald and C. Wunsch, *Nature* **382**, 436 (1996); C. Wunsch, D. Hu, B. Grant, *J. Phys. Oceanogr.* **13**, 725 (1983).
4. H. M. Stommel [*Tellus* **13**, 224 (1961)] was the first to use this approximation. See D. G. Wright and T. Stocker, *J. Phys. Oceanogr.* **21**, 1713 (1991); R. X. Huang, J. R. Luyten, H. M. Stommel, *ibid.* **22**, 231 (1992); and S. M. Griffies and E. Tziperman, *J. Climate* **8**, 2440 (1995) for more recent examples.
5. W. Munk, *J. Meteorol.* **7**, 79 (1950).
6. D. G. Wright, T. F. Stocker, and D. Mercer [*J. Phys. Oceanogr.* **28**, 791 (1998)] provide a comprehensive discussion of this issue in zonally averaged climate models. T. M. C. Hughes and A. Weaver [*ibid.* **24**, 619 (1994)] provide evidence for a relation between meridional pressure gradient and overturning strength in a GCM. An alternative explanation to the frictional explanation is to suppose that some portion of the eastward geostrophic transport associated with the pressure gradient is converted to overturning, as supposed by Bryan [in (*1*)].
7. The flow will be off to the left of the wind stress, because the Coriolis force acting on this velocity will balance the surface stress; see J. F. Price, R. A. Weller, R. R. Schudlich, *Science* **238**, 1534 (1987) for observations of such flow.
8. P. R. Gent and J. C. McWilliams, *J. Phys. Oceanogr.* **20**, 150 (1990); P. Gent, J. Willebrand, T. J. McDougall, J. C. McWilliams, *ibid.* **26**, 463 (1995); and G. Danabasoglu, J. C. McWilliams, P. R. Gent, *Science* **264**, 1123 (1994) document the effect of this parameterization on the global temperature and salinity structure.
9. W. Munk, *Deep-Sea Res.* **13**, 707 (1966).
10. D. Olbers and J. Wenzel [in *Ocean Circulation Models: Combining Data and Dynamics*, D. Anderson and J. Willebrand, Eds. (Kluwer, Dordrecht, Netherlands, 1989), pp. 99–140] estimate values for A_I between 100 and 1000 m^2 s^{-1}. These values are substantially lower than the 2000 to 3000 m^2 s^{-1} estimated by G. Holloway [*Nature* **323**, 243 (1986)] from observed sea surface height variability. J. Ledwell, A. Watson, and C. S. Law [*J. Geophys. Res.* **103**, 21499 (1998)] also found large values of A_I ($\sim$1000 m^2 s^{-1}) in the relatively quiet subtropical gyre.
11. The pycnocline depth z_σ is computed by defining

$$z_\sigma = \int_{z=-H}^{0} \Delta\sigma_2 \, z \, dz \bigg/ \int_{z=-H}^{0} \Delta\sigma_2 \, dz$$

where H is the depth, $\Delta\sigma_2 = \sigma_2(z) - \sigma_2(\text{max})$, and σ_2 is the potential density referenced to 2000 m. Pycnocline depths are computed from 50°W to 70°W and 40°S to 40°N in the Atlantic Basin.
12. See, for example, W. J. Schmitz and M. S. McCartney, *Rev. Geophys.* **33**, 151 (1993).
13. J. Ledwell, A. Watson, C. S. Law, *Nature* **364**, 701 (1993).
14. J. R. Toggweiler and B. Samuels, in *The Global Carbon Cycle*, M. Heimann, Ed. (Springer-Verlag, Berlin, 1993), pp. 303–331.
15. W. Munk and C. Wunsch [*Deep-Sea Res. Part I Oceanogr. Res. Pap.* **45**, 1977 (1998)] discuss this issue in detail.
16. The model used here is the GFDL Modular Ocean Model Version 3.0 documented in R. C. Pacanowski and S. M. Griffies, *GFDL Tech. Rep. 3* (Geophysical Fluid Dynamics Laboratory, Princeton, NJ, 1998). The grid spacing and bottom topography for this model are identical to those used in Toggweiler and Samuels (*17*). The surface winds are taken from S. Hellermann and M. Rosenstein, *J. Phys. Oceanogr.* **13**, 1093 (1982). Surface salinities are restored toward the climatological observations of Levitus (*2*), whereas surface temperatures are restored toward the data set that was used to drive the Atmospheric Model Intercomparison Project (AMIP) runs as described in W. L. Gates, *Bull. Am. Meteorol. Soc.* **73**, 1962 (1992).
17. J. R. Toggweiler and B. Samuels, *J. Phys. Oceanogr.* **28**, 1832 (1998).
18. This work was supported by the Carbon Modeling Consortium, NOAA grant NA56GP0439, and by the Geophysical Fluid Dynamics Lab. I thank A. Gnanadesikan and T. Hughes for extensive help with the text and model runs, and H. Bjornsson, R. Toggweiler, K. Bryan, and R. Hallberg for useful discussions. This paper is dedicated to the memory of Tertia Hughes.

30 December 1998; accepted 26 February 1999